· Review ·
doi: 10.13679/j.advps.2016.4.00219

Advances in Polar Science
December 2016 Vol. 27 No. 4: 219-232

Recent progress in Chinese polar upper-atmospheric physics research: review of research advances supported by the Chinese Arctic and Antarctic expeditions

HE Fang*, HU Hongqiao, YANG Huigen, ZHANG Beichen, HUANG Dehong, LIU Yonghua, HU Zejun & LIU Jianjun

SOA Key Laboratory for Polar Science, Polar Research Institute of China, Shanghai 200136, China

Received 15 November 2016; accepted 25 December 2016

Abstract It has been more than 30 years since the first Chinese Antarctic Expedition took place. Polar upper atmospheric observations started at this time. First began at Great Wall Station and then at Zhongshan Station in Antarctica, and later in the Arctic at Yellow River Station, Kjell Henriksen Observatory on Svalbard, and at the China-Iceland Joint Aurora Observatory in Iceland. In this paper, we reviewed the advances in polar upper atmosphere physics (UAP) based on the Chinese national Arctic and Antarctic research over the last five years. These included newly deployed observatories and research instruments in the Arctic and Antarctic; and new research findings, from ground-based observations, about polar ionosphere dynamics, aurora and particle precipitation, polar plasma convection, geomagnetic pulsations and space plasma waves, space weather in the polar regions, simulations of the polar ionosphere-magnetosphere. In conclusion, suggestions were made for future polar upper atmosphere physics research in China.

Keywords **upper-atmospheric physics, research advances, polar ionosphere, aurora, particle precipitation, plasma convection, plasma waves, space weather**

Citation: He F, Hu H Q, Yang H G, et al. Recent progress in Chinese polar upper-atmospheric physics research: review of research advances supported by the Chinese Arctic and Antarctic expeditions. Adv Polar Sci, 2016, 27: 219-232, doi:10.13679/j.advps.2016.4.00219

1 Introduction

The upper atmosphere is the region of outer space near Earth that includes the magnetosphere, which is affected by solar activity. Intense solar activity such as solar storms can cause severe space weather, which could obstruct aviation communications, disturb navigation signals, and damage power grids/facilities.

In polar regions, geomagnetic field lines are aligned approximately perpendicularly to the ground plane. Energetic particles from the solar wind that are energized at the magnetopause or in the magnetotail can penetrate the magnetosphere and middle atmosphere along geomagnetic field lines and arrive at relatively low altitudes. As Earth's window to outer space, the upper atmosphere of the polar regions has considerable importance. Some phenomena such as auroras, substorms, polar cap absorption, and aurora absorption occur exclusively in this area, but related effects might appear subsequently in mid- and low-latitude regions. Therefore, the work of monitoring and investigating the geophysical phenomena that occur in the polar upper atmosphere is important in relation to forecasting the geospatial environment.

Chinese polar research activities in Antarctica have been performed since 1984, and China's first permanent station in the Arctic has been operational since 2004. Some of China's earlier research advances in polar upper-atmospheric physics (UAP) have been reviewed by Liu and Yang[1]. In this paper, the observation sites and instruments deployed by China in the past 5 years to further polar upper-atmosphere research are introduced, relevant research findings are reviewed, and future research prospects are considered.

* Corresponding author, E-mail: hefang@pric.org.cn

2 Observational systems of polar upper-atmospheric physics

Chinese polar UAP studies are based mainly on observational data obtained from three permanent polar stations: Great Wall Station (GWS) and Zhongshan Station (ZHS) in Antarctica, and Yellow River Station (YRS) in the Arctic.

The GWS is located on King George Island of the Antarctic Peninsula in the area of the Weddell Sea Anomaly (WSA) and the South Atlantic Anomaly. Because of its relatively low geographic latitude (48.4°), GWS travels within the subauroral region. It is China's only site in the Western Hemisphere for monitoring the space environment. The observation elements of UAP at GWS are focused on the ionosphere and geomagnetic field. Since March 2013, a set of tri-band beacon receivers has been deployed at GWS for polar ionospheric environment monitoring by the China Research Institute of Radio Wave Propagation. The tri-band beacon receivers are able to receive satellite signals on multiband frequencies (VHF, UHF, and L-band), which can be used to deduce information on the total electron content (TEC), scintillation of the ionosphere, and structure of irregularities. With the operating GPS receivers, the capability for monitoring small-scale irregularities at GWS has been improved.

The invariant geomagnetic latitude of ZHS is about 74.8°, which means it is located in the cusp region during magnetic noon and in the polar cap region during magnetic night. The ZHS passes through the auroral zone twice daily, which makes it a very suitable site at which to perform observations of the magnetosphere, ionosphere, and aurora for the study of solar-terrestrial energy transportation processes, especially for post-noon auroral observations. At present, the UAP observation instrumentation at ZHS consists of an auroral spectrometer, three specific wavelength (427.8, 557.7, and 630.0 nm) auroral imagers, an induction magnetometer, a fluxgate magnetometer, an imaging riometer, a cosmic ray muon telescope, a digisonde, a Super Dual Auroral Radar Network (SuperDARN) high-frequency (HF) coherent scattering radar, and three ionosphere scintillation/TEC monitors.

The invariant geomagnetic latitude of YRS is about 76.5°. The station is located at Ny-Ålesund in Svalbard (geographic coordinates: 78.9°N, 11.9°E). Because of its high latitude, the duration of the polar night at YRS can persist for more than three months, which makes the station ideal for continuous dayside auroral observations. Moreover, the geomagnetic position of YRS is approximately conjugate with that of ZHS. The similarity between the scientific observation instrumentation deployed at the two stations favors high-latitude magnetic conjugacy studies. Currently, the UAP observation instrumentation at YRS comprises three specific wavelength (427.8, 557.7, and 630.0 nm) auroral imagers, an auroral spectrometer, a Fabry–Perot interferometer, an induction magnetometer, a fluxgate magnetometer, an imaging riometer, and three ionosphere scintillation/TEC monitors. The instruments at ZHS and YRS comprise an advanced polar UAP conjugacy observation pair at the latitude of the cusp region. Scheduled routine observations have been performed continuously since the installation of the instrumentation. Thus, conjugacy data have been obtained over a 13-year period from winter 2004 to spring 2017.

Following increased funding for polar UAP research, the Polar Research Institute of China (PRIC) established a new observatory by renting a laboratory at the Kjell Henriksen Observatory (KHO) of the University Centre in Svalbard in 2011. It is equipped with a six-wavelength (427.8, 432.0, 540.0, 557.7, 620.0, and 630.0 nm) filter-wheel auroral imager and a fluxgate magnetometer. The KHO is only about 100 km from YRS; thus, the proximity of these two stations makes it possible to undertake dual-station auroral observations to acquire three-dimensional aurora images.

In September 2013, the PRIC and the Icelandic Centre for Research signed an agreement on the formation of a joint center for the exploration of the Aurora Borealis. The aim of this cooperative research is to further scientific understanding of solar-terrestrial interaction and space weather by conducting polar upper-atmospheric observations of auroras, geomagnetic field variations, and other related phenomena and to provide outreach to the public. After consideration of a number of factors, it was determined that the China-Iceland Joint Aurora Observatory (CIAO) should be located at Karholl in northern Iceland. The CIAO is located at 65.7°N, 17.4°W with an invariant geomagnetic latitude of 65.5°. This geomagnetic latitude means CIAO is situated within the nightside auroral oval. It is anticipated that CIAO will observe space weather activities such as auroras, magnetic storms, and substorms. The observational instruments already in operation at CIAO include a six-wavelength (427.8, 432.0, 540.0, 557.7, 620.0, and 630.0 nm) filter-wheel auroral imager and a fluxgate magnetometer. An imaging riometer is under construction, which will begin field trials in 2017. Other instruments scheduled for implementation in the near future include an ionosphere scintillation/TEC monitor, an ELF/VLF receiver, and three specific wavelength (427.8, 557.7, and 630.0 nm) auroral imagers.

The geographic and corrected geomagnetic coordinates of the five polar UAP observatories are listed in Table 1, and

Table 1 Geographic and corrected geomagnetic coordinates of GWS and ZHS in Antarctica, and YRS, CIAO, and KHO in the Arctic

Stations	Geographic coordinates		CGM coordinates(2015)	
	Latitude	Longitude	Latitude	Longitude
GWS, Antarctica	62.22°S	58.96°W	-48.40°	11.85°
ZHS, Antarctica	69.37°S	76.38°E	-74.83°	98.23°
YRS, Svalbard	78.92°N	11.93°E	76.54°	108.47°
CIAO, Iceland	65.70°N	17.36°W	65.52°	70.08°
KHO, Svalbard	78.21°N	15.71°E	75.80°	109.18°

the details of the on-site UAP observational instrumentation are listed in Table 2.

In addition to the hardware installations, data processing platforms have been designed and implemented, e.g., the auto aurora arc interpretation system and the induction magnetometer data analysis system. Furthermore, the Digisonde ionogram interpretation and drift data analysis tools have been updated. Some of the ionospheric and geomagnetic

Table 2 On-site UAP observational instruments at the five polar stations listed in Table 1

Stations	Instruments	Observing parameters	Sampling mode	Observing period
GWS, Antarctica	Ionosphere scintillation/ TEC monitors	Total electron content in ionosphere, ionosphere S4 scintillation index	Routine operation, continuous passive receiving per second	All day long since 2008
	Tri-band beacon receivers	Total electron content in ionosphere, ionosphere S4 scintillation index	Routine operation, continuous passive receiving per second	All day long since 2010
ZHS, Antarctica	Digisonde	Ionogram, plasma drift velocity	Routine operation, continuous scanning every 7.5 min	All day long since 1995
	HF coherent scattering radar	Radial velocity of ionospheric patches, spectrum broadening, radar echo amplitude	Routine operation, continuous scanning every 3 min	All day long since 2010
	Imaging riometer	2D ionosphere absorption values of the cosmic noise at 38 MHz	Routine operation, continuous passive receiving per second	All day long since 1998
	Ionosphere scintillation/ TEC monitors	Total electron content in ionosphere, ionosphere S4 scintillation index	Routine operation, continuous passive receiving per second	All day long since 2010
	3 wavelengths aurora CCD imager system	2D aurora intensity for specific wavelength of 427.8, 557.7 and 630.0 nm	Continuous capturing every 10 s during dark night with fine weather.	In austral polar night since 2010
	Aurora spectrograph	Aurora spectrum intensity along the geomagnetic N-S meridian line	Continuous capturing every 20 s during dark night with fine weather.	In austral polar night since 2010
	Induction magnetometer	Relative variation of geomagnetic *H* and *D* components	Routine operation, sampling rate: 0.5–2 Hz	All day long since 1995
	Fluxgate magnetometer	Relative variation of geomagnetic *X*, *Y* and *Z* components	Routine operation, sampling rate: 1 Hz	All day long from 1995 to 2006, and from 2012 up to now
YRS, Svalbard	Ionosphere scintillation/ TEC monitors	Total electron content in ionosphere, ionosphere S4 scintillation index	Routine operation, continuous passive receiving per second	All day long since 2006
	3 wavelengths aurora CCD imager system	2D aurora intensity for specific wavelength of 427.8, 557.7 and 630.0 nm	Continuous capturing every 10 s during dark night with fine weather.	In boreal polar night since 2003
	Aurora spectrograph	Aurora spectrum intensity along the geomagnetic N-S meridian line	Continuous capturing every 20 s during dark night with fine weather.	In boreal polar night since 2013
	Imaging riometer	2D ionosphere absorption values of the cosmic noise at 38.235 MHz	Routine operation, continuous passive receiving per second	All day long since 1991
	Induction magnetometer	Relative variation of geomagnetic *H* and *D* components	Routine operation, sampling rate: 0.5–2 Hz	All day long since 2014
	Fluxgate magnetometer	Relative variation of geomagnetic *X*, *Y* and *Z* components	Routine operation, sampling rate: 1 Hz	All day long since 2016
KHO, Svalbard	Filter-Wheel with 6 wavelengths all sky CCD imager	2D aurora intensity for specific wavelength in sequence of 427.8, 432.0, 540.0, 557.7, 620.0, 630.0 nm	Continuous capturing every 10 s during dark night with fine weather in sequence of 427.8, 432.0, 540.0, 557.7, 620.0, 630.0 nm	In boreal polar night since 2011
	Fluxgate magnetometer	Relative variation of geomagnetic *X*, *Y* and *Z* components	Routine operation, sampling rate: 1 Hz	All day long since 2014
CIAO, Iceland	Filter-wheel with 6 wavelengths all sky CCD imager	2D aurora intensity for specific wavelength in sequence of 427.8, 432.0, 540.0, 557.7, 620.0, 630.0 nm	Continuous capturing every 10 s during dark night with fine weather in sequence of 427.8, 432.0, 540.0, 557.7, 620.0, 630.0 nm	In boreal polar night since 2014
	Fluxgate magnetometer	Relative variation of geomagnetic *X*, *Y* and *Z* components	Routine operation, sampling rate: 1 Hz	All day long since 2015
	Imaging riometer	2D ionosphere absorption values of the cosmic noise at 38.235 MHz	Routine operation, continuous passive receiving per second	Under construction, start running in 2018

data sets have been released online and they are available via http://www.chinare.org.cn/.

3 Research advances in the last 5 years

Polar UAP research is one of the main subjects of polar research. A series of national research projects has been dedicated to this subject continuously in China over the last 5 years. The research interests are focused primarily on the characteristics of the polar ionosphere, auroral and magnetospheric activities at high latitudes, and the interactions between them.

3.1 Polar ionosphere

Ionospheric electron density is an important parameter that can have many effects on the radio waves that propagate into the ionosphere. Xu et al.[2] examined the climatological features and solar activity dependences of the ionospheric F2-layer peak electron density (NmF2) using long-term observations from the Arctic and Antarctic stations of Tromsø, Longyearbyen, and ZHS. Diurnal and annual variations of NmF2 at geomagnetic/geographic conjugate stations at cusp/auroral latitudes were investigated and compared. It was found that the peak time of NmF2 at the three stations differed, indicating the importance of soft particle precipitation and ionospheric convection in the cusp region. Enhancement of NmF2 was detected at magnetic midnight in winter at Tromsø, which was believed caused by nighttime substorms.

In order to check the variability of NmF2 at ZHS in Antarctica, and at Longyearbyen and YRS in the Arctic, and its relationship with solar activity, He et al.[3-4] and Xu et al.[5] analyzed observational results and compared them with the predicted International Reference Ionosphere 2007 (IRI-2007) values. The long-term observational results at the three stations are shown in Figure 1. The comparison indicated that the IRI prediction performed well in the daytime but that it was much poorer in the dark time of the polar night. It meant that the IRI-2007 model reproduced the F2 peak parameters dominated by solar photoionization reasonably well, but that it did not address the effects of electron precipitation; hence, the discrepancies became large in the winter ionosphere.

As phenomena occurring frequently during summer days in the high-latitude ionosphere, *F*-lacunae are manifest as disappearances in F region ionogram traces. Based on the 7.5-min-interval Digisonde ionograms recorded at ZHS, Yang et al.[6] presented the temporal characteristics of *F*-lacunae, as well as their correlation with geomagnetic activity, the interplanetary magnetic field, and collocated TEC. It was reported that the Magnetic Local Time (MLT) distribution of *F*-lacuna occurrence exhibited dawn–dusk asymmetry. All types of *F*-lacuna favored the dawn sector, occurring mainly at 08:00–11:00 MLT for *F*1 and total lacunae and at 06:00–8:00 MLT for *F*2-lacunae. Magnetic activity was found to have strong positive correlation with *F*2 and total lacunae. *F*2-lacuna occurrence was favored by the southward component of the interplanetary magnetic field (IMF), and total lacuna occurrence was favored by high values of either eastward or westward components. *F*-lacunae are associated with the simultaneous TEC condition, which has positive correlation with *F*1-lacuna occurrence and strong negative correlation with the occurrence of *F*2 and total lacunae. The associated TEC variation might provide significant evidence for interpreting *F*-lacuna phenomena. Yang et al.[7] later studied the rate of occurrence of all three types of *F*-lacuna under different conditions of solar wind velocity based on *F*-lacuna events with manual judgements. Statistical analysis of the daily frequency of *F*-lacuna occurrence in relation to averaged solar wind velocity indicated that *F*2-lacunae occurred more frequently with higher solar wind velocity.

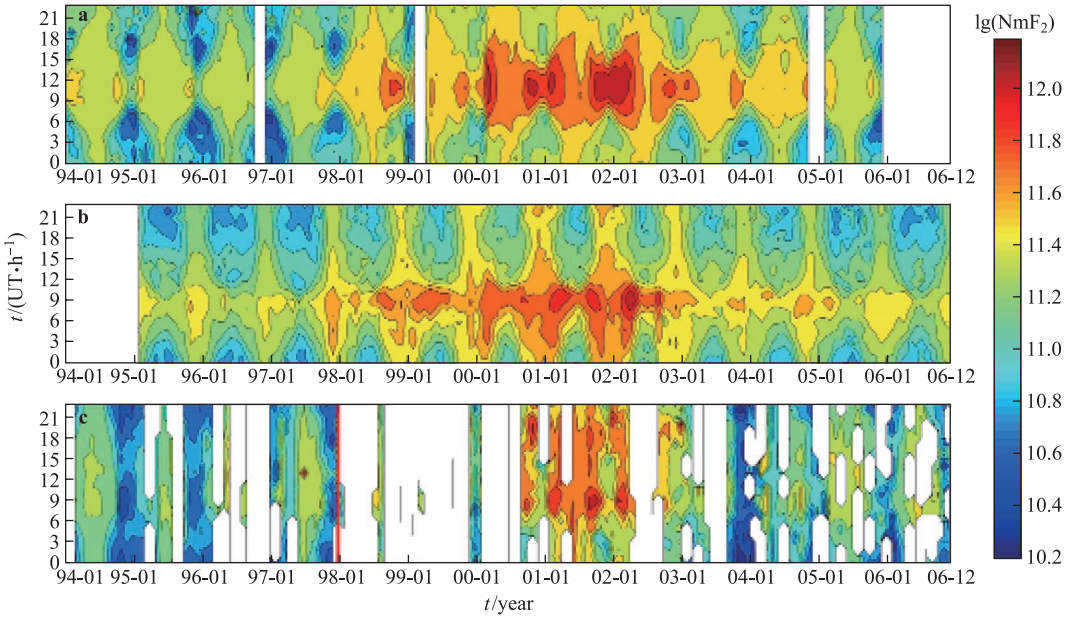

Figure 1 NmF2 contour plots: (**a**) Tromsø, (**b**) Longyearbyen, and (**c**) ZHS (from 1994 to 2006)[2].

The E-layer Dominated Ionosphere (ELDI) is a polar ionospheric phenomenon of electron enhancement in the E layer. The characteristics of the ELDI in the Antarctic during the polar night were investigated and compared with the Arctic by Wu et al.[8] They found that the ELDI was obvious in the polar region during the polar night and that its distribution was very similar to that of the auroral oval. The occurrence of the ELDI was higher on the night side, by about 70% in the Arctic and by 90% in the Antarctic, and it was caused mainly by the precipitation of high-energy particles. The difference in the distributions between the Antarctic and the Arctic might be caused by the separation of the geomagnetic pole from the geographic pole in the two regions. Moreover, the characteristics of the temporal variations of ELDI intervals were investigated using field-aligned measurements from the European Incoherent Scatter Scientific Association (EISCAT) radars and EISCAT Svalbard Radar (ESR) during 2009–2011[9]. It was found that ELDIs were observed more often in winter and early spring than in other seasons, especially in the auroral zone. The occurrence of ELDI intervals peaked around geomagnetic midnight at auroral latitudes, while it reached a maximum around geomagnetic local noon at the latitude of the ESR. This implied that ELDI intervals are sporadic rather than regular phenomena.

In lower ionospheric investigations, cosmic noise is often used as a natural indicator for radio absorption effects of high-frequency bands. Cosmic noise absorption (CNA) occurs mostly in the D region of the lower ionosphere. He et al.[10] suggested a new technique for estimating the quiet-day curve (QDC), which is vital for generating a reasonable CNA curve. To validate the new approach, QDCs were derived from data acquired by the imaging riometer installed at ZHS. The evaluation was performed by comparing the difference between QDCs derived by the new technique and those derived by Tanaka's technique[11]. The results were discussed in terms of diurnal variation and discrepancy. The findings suggested that the QDC generation technique was appropriate for imaging riometers located at other sites in the polar region of both hemispheres. Based on this technique, observation results from the imaging riometer at ZHS have been reported[12] for the solar event on 12–14 July 2012. CNA keograms (time–latitude displays created from imaging photometer data) were built and analyzed. It was found that *in situ* auroral keograms had movement similar to CNA curves. The interplanetary shock caused by the same solar event was also studied by Liu et al.[13] using observations from SuperDARN, the International Monitor for Auroral Geomagnetic Effects (IMAGE) magnetometer chain in the Northern Hemisphere, and all-sky auroral Images from ZHS. The data from the conjugated stations showed significant ionospheric responses to the solar event at both stations. However, the observation discrepancy between the two was attributed primarily to the different solar radiation conditions.

Based on scintillation receiver observations from December 2013 to November 2014 at the South Pole and McMurdo stations, statistical analyses were performed on the diurnal and seasonal variations of phase scintillation occurrence at the two stations[14]. The results indicated that phase scintillation occurrence in spring and autumn was significantly greater than in summer and winter, and that the diurnal variation exhibited a twin-peaked structure. Enhanced occurrence of scintillation at magnetic post-midnight could be induced by a strong density gradient caused by the plasma cloud across the polar cap region.

To analyze the characteristics of TEC variation in the polar ionosphere, the Global Navigation Satellite System (GNSS) has been used to generate key ionospheric parameters. Based on over 40 GNSS tracking stations deployed by the International GNSS Service (IGS), Polar Earth Observing Network (POLENET), and Chinese Antarctic Center of Surveying and Mapping in Antarctica, an ionospheric tomography model applicable in Antarctica has been developed[15]. Using this model, the electron density and TEC were deduced and the full evolution of the "tongue" of ionization (TOI), including its formation, evolution, transition, and decay, has been studied. Based on GPS signal data, An et al.[16] analyzed the characteristic of TEC variation in southwest Antarctica and they studied the WSA. The WSA occurs mainly in the coastal region in summer, and it can be characterized by electron density enhancement during midnight. Long-term observations of GPS signal data in the Arctic and the Antarctic regions have been analyzed together with IGS data, and the characteristics of the spatiotemporal distributions of TEC in both polar regions have been studied. The results are important for understanding the morphological characteristics of the polar ionosphere[17-18]. Deng et al.[19] also investigated the variations of ionospheric TEC surrounding GWS using GPS data. Their results showed that when the WSA could be observed, the TEC value was higher on the nightside than the dayside in summer. Up to 94.8% of TEC storm events were accompanied by intense disturbances of the AE index. It suggested there is strong correlation between auroral substorms and TEC storms.

3.2 Aurora and particle precipitation

The aurora is one of the most significant visible manifestations of the dynamic processes associated with the precipitation of particles into the polar ionosphere generated by solar–terrestrial interactions. Auroral studies have played an important role both in developing our understanding of Earth's environment and in improving our ability to predict space weather. The different features of auroral forms reflect the various physical processes operating in the magnetosphere.

Poleward moving auroral forms (PMAFs) were investigated statistically using continuous, high-quality, optical observations obtained from three-wavelength all-sky imagers at YRS over six winters[20]. In particular, the dependence of PMAF occurrence on solar wind conditions during 09:00–15:00 MLT was examined. It was found that 59%, 60%, and 57% of PMAF events occurred under IMF conditions of negative B_z, positive B_y, and negative B_x, respectively, where

B_z, B_y, and B_x represent the triaxial components of the vector quantity B of the IMF. The PMAFs showed a tendency to occur preferentially under large IMF $|B_x|$ conditions. The MLT dependence of PMAFs presented remarkable reduction in the midday sector, showing clear IMF B_y-related pre-noon–post-noon asymmetry, consistent with the motion of reconnected flux tubes due to the release of magnetic field tension. The statistical results suggested PMAFs are not caused by pressure pulses of the solar wind but by bursts of magnetic reconnection. Using optical data with high temporal resolution, obtained from the three-wavelength all-sky imagers at YRS, together with particle precipitation data from the Defense Meteorological Satellite Program, Xing et al.[21] investigated the quantitative relationship between auroral intensities and the energy features of precipitated particles near magnetic noon. Their results indicated that soft auroral electron precipitation dominated near magnetic noon during 10:00–13:00 MLT. A model of auroral emissions and particle precipitation near magnetic noon at YRS has been developed. Xing et al.[22] also performed a statistical investigation of the dependence of the location of PMAFs on the IMF B_z and B_y components as a function of MLT and geomagnetic latitude (MLAT) under stable IMF conditions. It was found that PMAFs occurred more frequently at lower latitudes for $B_z < 0$, and there was less evident IMF B_y-related pre-noon–post-noon asymmetry for $B_z < 0$ than for $B_z > 0$. The PMAFs were distributed over a wide range of MLT when $B_z < 0$, which indicates the reconnection X-line might spread like an "S" shape. However, during a northward IMF, PMAFs were observed predominantly pre-noon for IMF $B_y > 0$ and post-noon for IMF $B_y < 0$, in association with the effects of high-latitude reconnection, consistent with the theoretical model of convection flow.

Using the polar ultraviolet imager (UVI) above the Arctic and the all-sky camera at ZHS in Antarctica, a hemispheric conjugate observation of post-noon "bright spots" in the Arctic and auroral spirals in Antarctica was presented by Hu et al.[23]. It was considered that the auroral spirals in post-noon arcs were the visible characteristics of post-noon UV bright spots in the ground-based observations. This suggested that current sheet instability above the parallel electric field region, which could produce the arcs, was the origin of the bright spots occurring in the ionosphere. Furthermore, it was claimed that the hemispheric symmetry/asymmetry of post-noon upward field-aligned currents, which are affected by the IMF B_y and season, could control the conjugacy/nonconjugacy of post-noon bright spots/auroral spirals between the two hemispheres. Subsequently, Hu et al.[24] also performed a comprehensive analysis of long-term and multispectral auroral observations made in the Arctic and in Antarctica. They demonstrated that the dayside auroral ovals in the two hemispheres both presented two-peaked structures, i.e., the pre-noon 09:00 MLT and post-noon 15:00 MLT peaks. The two-peaked structures of the dayside ovals, however, were asymmetric in the two hemispheres. This hemispheric asymmetry could not be explained by the effects of the IMF B_y component or the seasonal differences in ionospheric conductivities between the two hemispheres, which have been used to interpret satellite-derived real-time auroral intensity asymmetries in the two hemispheres in previous studies. It was suggested that hemispheric asymmetry reflects the combined effects of pre-noon–post-noon variations of the magnetosheath density and local ionospheric conductivity.

The dayside diffuse aurora (DDA) is an auroral form observed exclusively by the all-sky imagers at YRS. During 05:00–13:00 MLT on 2 January 2006, the intensity of the DDA was highly correlated with the solar wind dynamic pressure (max. coefficient: 0.89)[25]. Moreover, there were similar spectral characteristics in the Pc5 (the Type 5 continuous pulsation of geomagnetic pulsations) range between the intensity of the DDA and the solar wind dynamic pressure during the portion of the observation period when the IMF B_z was northward. This observation indicates that changes in the solar wind dynamic pressure could efficiently modulate the magnitude of the DDA, except when the IMF is southward. Enhancement of the solar wind dynamic pressure could provide favorable circumstances for dayside chorus wave generation, and the dayside chorus wave could be a candidate for the production of DDAs.

Using optical auroral observations obtained at YRS over 7 years, Han et al.[26] performed the first extensive survey of DDAs and they reported the following results. (1) DDAs can be classified broadly into two categories: unstructured and structured. (2) Unstructured DDAs observed in the morning and the afternoon present obviously different properties. Afternoon DDAs are much more stable and they seldom show pulsating properties. (3) DDAs are observed more easily under geomagnetically quiet conditions. (4) Structured DDAs show patchy, stripy, and irregular forms and they are often pulsating and drifting. The drift directions are mostly westward (with speeds of approximately 5 km·s^{-1}), but cases showing eastward or poleward drift have been observed. (5) Stripy DDAs are observed exclusively near magnetic local noon (MLN) and their alignments are consistent with the direction of ionospheric convection near MLN. (6) A new auroral form, called throat aurora, was found to develop from stripy DDAs. Figure 2 shows the possible mechanism of generation of DDAs in the morning, at MLN, and in the afternoon. It suggests that unstructured DDAs observed in the morning are extensions of nightside diffuse aurora to the dayside, but that DDAs observed in the afternoon are caused predominantly by proton precipitation. The throat aurora is considered a projection of a newly opened flux of reconnection.

It is suggested that the throat aurora is generated by magnetospheric cold plasma flowing into the magnetopause reconnection site; thus, it represents an ionospheric signature of a newly opened flux of reconnection. By examining simultaneous low-altitude-satellite and ground-based observations, Han et al.[27] confirmed that throat auroras were associated with low-energy electrons and ion precipitation

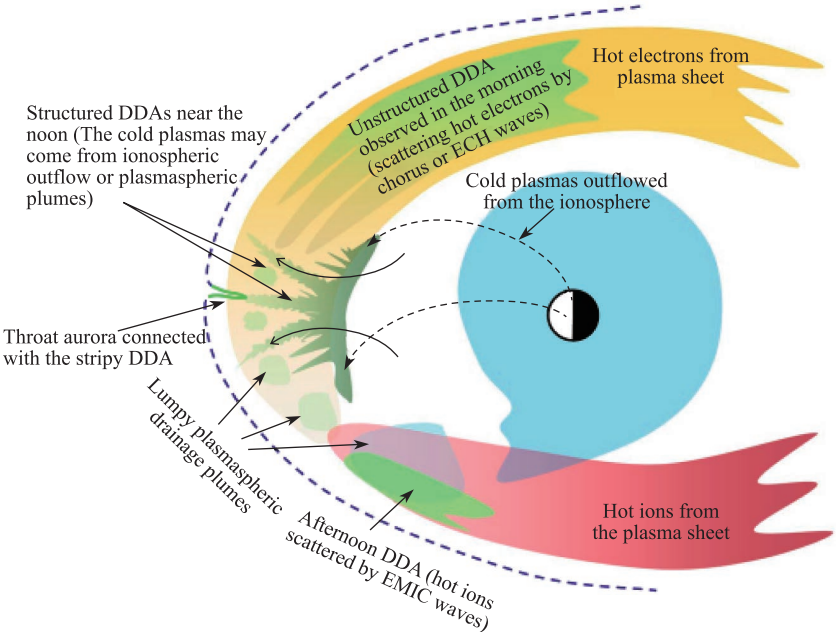

Figure 2 Schematic showing the mechanism of generation of DDAs observed in the morning, at MLN, and in the afternoon[26].

of magnetosheath type, providing the first evidence that they occur along open magnetic field lines. Additionally, the observations had other important implications: (1) solar wind particles could penetrate deep into the magnetosphere and therefore, they might make significant contributions to the low-energy plasma often observed in the dayside outer magnetosphere, and (2) localized shapes of the magnetopause and the ionospheric open–closed field line boundary might be changed substantially during the generation of throat aurora. Using the seven-year continuous auroral observations obtained at YRS, Han et al.[28] investigated the observational properties of throat aurora in detail. It was found that throat auroras are always observed together with diffuse auroras, which indicates their occurrence is affected by factors within the magnetosphere. However, the rate of occurrence of throat auroras decreases with the increase of the IMF cone angle, implying their occurrence is affected by external factors.

Qiu et al.[29] investigated the orientations of dayside auroral arc alignments for over 40000 all-sky images obtained at YRS. For each arc, its "orientation" and "tilt" were defined as the angles made by the arc alignment with the dusk–dawn direction and the local east–west direction, respectively. The mean arc orientation increased linearly with increasing MLT. It was found that the reversal position shifted toward the midday for negative B_y. Qiu et al.[30] also found that the velocity of the auroral arc was determined by the distance of the arc away from the zenith and the arc tilt. The arc tilt determined the velocity orientation and it was found to be most important. Furthermore, equatorward motion of the arc was much more evident than poleward motion.

Recently, Ni et al.[31] reviewed the latest advances both in our understanding of the origin of diffuse aurora and in our ability to quantify the exact roles of various magnetospheric waves in producing the global distribution of diffuse auroral precipitation and of its variability in relation to geomagnetic activity.

The nightside aurora, the energy of which is derived from the magnetotail, is more commonly observed at ZHS and YRS. Liu et al.[32] analyzed the response of nightside auroras to the interplanetary shock of sudden compression using ground-based optical aurora observations from ZHS and YRS. They found 18 shock-associated auroral cases that indicated nightside aurora responses could be classified into auroral breakup and weak intensification or null events. Epoch time analysis showed that both the coupling efficiency of the solar wind and the magnetosphere and the electromagnetic environment within the magnetosphere determined the nightside aurora response. Using ground-based high temporal and high spatial resolution optical aurora observations, Liu et al.[33] investigated one fortuitous event that occurred on 7 January 2005 to illustrate the direct response of the fine structure of the auroral emission to interplanetary shock. The observations showed that an intensified red aurora, which manifested as a discrete emission band at higher latitudes, responded gradually to the shock impact. This resulted in a distinct broadening of the dayside auroral oval due to the equatorward shift of its lower latitude boundary after the shock arrival. In contrast, a green diffuse aurora, which manifested as a structure with relatively uniform luminosity, reacted immediately to the shock compression, displaying prompt appearance at the southern edge of the field of view and subsequent poleward propagation of its higher latitude boundary. These direct observations strongly suggest that prompt shock compression intensifies wave-particle interactions in the inner magnetosphere and enhances the lobe magnetic reconnection rate at magnetospheric high latitudes.

At the end of 2014, a dual-detector cosmic ray muon telescope with a 0.5 × 0.5 m scintillator was deployed at ZHS. Huang et al.[34] reported that the telescope data showed

significant effects of atmospheric pressure change with negative correlations. The vertical cutoff rigidity of cosmic ray protons at ZHS is 0.076 GV, making ZHS a suitable location for the observation of solar proton events.

3.3 Polar plasma convections

The interaction between the solar wind (and its IMF in particular) and Earth's magnetosphere causes large-scale plasma movement within the magnetosphere that appears as a permanent and highly variable plasma circulation in the high-latitude polar ionosphere.

To investigate the relationship between convection and solar activity, Zhang et al.[35] reported a number of backscatter power enhancement events with "equatorward-moving radar auroral forms" in the high-latitude ionosphere, which were observed by the SuperDARN CUTLASS (a bistatic HF coherent radar with stations in Finland and Iceland) Finland radar when the IMF was northward during 09:00–10:00 coordinated universal time (UTC) on 26 March 2004. These events were also associated with sunward flow enhancements at each location in the Northern Hemisphere, which were shown by ionospheric convection measured by the SuperDARN radars. These are typical features of high-latitude (lobe) magnetic reconnections. The durations of the velocity enhancements implied that the evolution time of the lobe reconnections was about 8–16 min from their origin at the reconnection site to their addition to the magnetotail lobe. In addition, the Double Star TC-1 spacecraft was moving from the magnetosheath into the magnetosphere, and crossing the magnetopause near the subsolar region during this interval, and it observed typical low-latitude magnetic reconnection signatures. Based on these observations, it was inferred that dayside high- and low-latitude reconnections might occur simultaneously.

Patches of ionization are common in the polar ionosphere, where their motions and associated density gradients cause variable disturbances to HF radio communications, over-the-horizon radar location errors, and disruption and errors to satellite navigation and communication systems. Their formation and evolution are poorly understood, particularly under disturbed space weather conditions. Zhang et al.[36] reported direct observations of the full evolution of such patches during a geomagnetic storm, including formation, polar cap entry, transpolar evolution, polar cap exit, and sunward return flow, as shown in Figure 3. The observations showed that modulation of nightside reconnection in the substorm cycle of the magnetosphere helped form the gaps between patches where steady convection could create a TOI.

Zhang et al.[37] also found two types of poleward-moving plasma concentration enhancement (PMPCE) during a sequence of pulsed reconnection events, both in the morning convection cell. Type L (low-density) PMPCEs were associated with a cusp flow channel and they appeared to have been produced by ionization associated with particle precipitation. Type H (high-density) PMPCEs appeared to originate from the segmentation of the TOI by the processes that produced the Type L events. Consequently, the Type L and Type H PMPCEs were interspersed, producing a complex density structure that underlined the importance of cusp flow channels as a mechanism for segmenting and structuring electron density in the cusp. Furthermore, it showed the necessity of distinguishing between at least two classes of electron density patch.

Zhang et al.[38] reported a clear transition through a reconnection layer at the low-latitude magnetopause, which showed a complete traversal across all reconnected field lines during northwestward IMF conditions. The associated plasma populations confirmed the details of the electron and ion mixing, and the time history and acceleration through the current layer. This case had low magnetic shear with a strong guide field, and the reconnection layer contained a single-density depletion layer on the magnetosheath side, which suggested nearly field-aligned magnetosheath flows.

To understand the evolution of TOI/patches/blobs, it is essential to examine how the transported sunlit plasma is distributed. Through averaging the hourly TEC in the solar-maximum winter, Yang et al.[39] presented a complete distribution of polar ionospheric plasma. They found that dayside plasma could be transported through the cusp, over the polar cap, and eventually to the prevailing dawnside, showing asymmetric distribution around magnetic midnight. The negative interplanetary magnetic field B_y or B_z component was favored for plasma transportation from the dayside to the prevailing dawn sector. This provided direct evidence for the plasma source of the dawnside high-density plasma structure. The same corotating convection direction as the convection at the auroral dawnside was responsible for the prevailing dawn sector transportation. This finding was significant for forecasting TOI/patches/blobs in conducting space weather studies in the polar ionosphere.

The diurnal variation of HF radar echoes and the associated influence of geomagnetic activity have been analyzed using HF radar data obtained at ZHS from April 2010 to February 2011 by Liu et al.[40]. The diurnal variation was very clear and the influence of geomagnetic activity was significant. The peak echo occurrence occurred at the dayside during geomagnetic quiet conditions, and it shifted toward the nightside and showed a declining trend with an increase in the level of geomagnetic activity. The results indicated that the average line-of-sight velocity has clear diurnal variation. At the nightside, the velocity was positive most of the time, indicating plasma was moving toward the radar; however, at the dayside, the velocity was negative, indicating plasma was moving away from the radar.

To study the trigger of the shock aurora, Liu et al.[41] presented observations of a duskside shock aurora event, which occurred on 21 April 2001, obtained by the SuperDARN radar at Syowa Station in Antarctica and the all-sky camera at ZHS when the radar was operated in fast-scan mode covering the ZHS region. Using these two independent data sets, they examined ionospheric plasma convection and

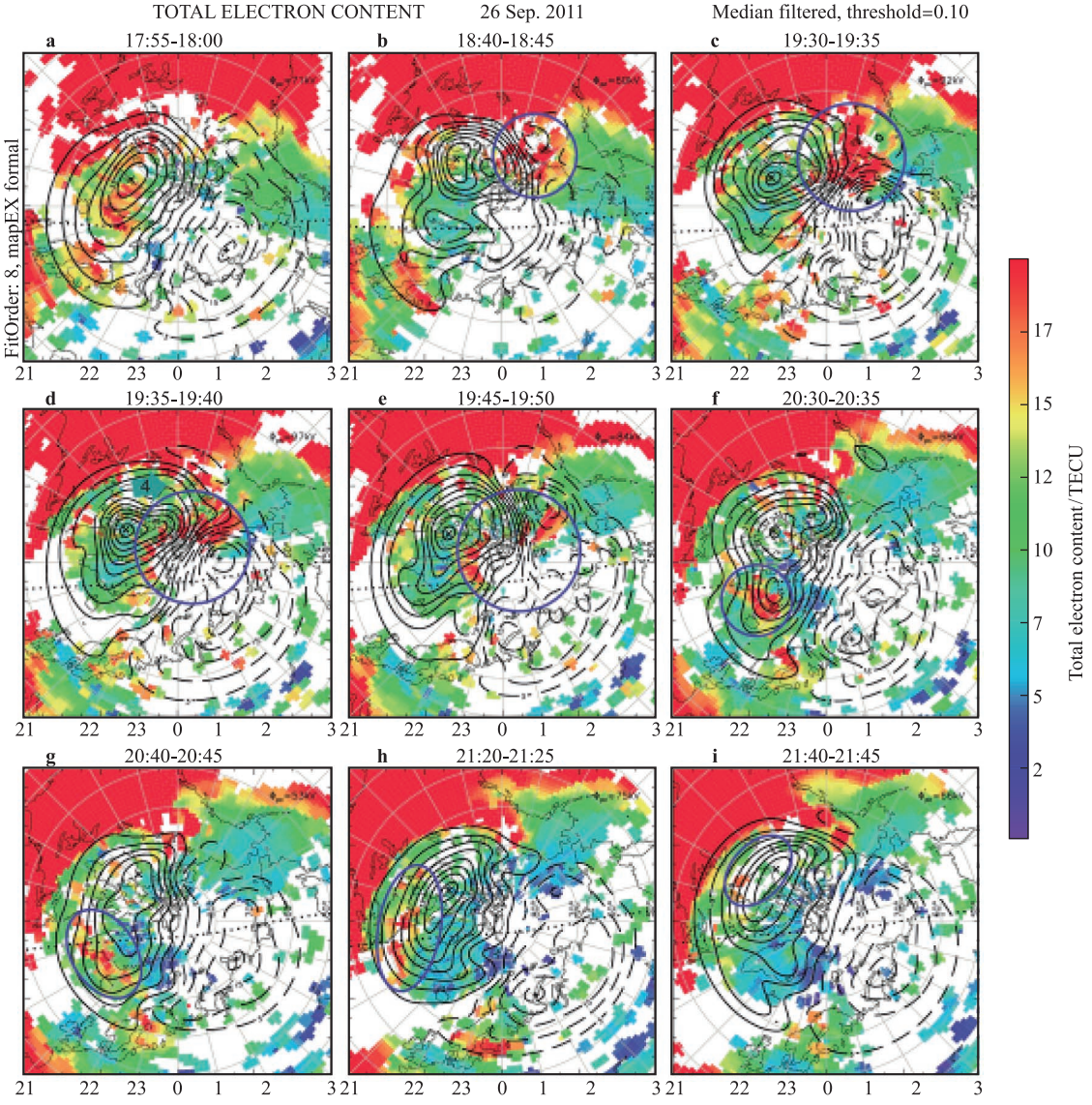

Figure 3 Extracts from a full series of 2D maps of median-filtered TEC and ionospheric convection on a geomagnetic latitude/MLT grid with noon at the top(**a**–**i**). The dotted line across each panel is the day–night terminator at 100-km altitude. The blue circles and ellipses highlight the polar cap patch, the evolution of which is followed in this figure[36].

aurora arising from a sudden impulse (SI) event associated with an interplanetary shock. The SuperDARN radar line-of-sight measurements showed periodic oscillation in the flow direction with ultralow-frequency waves with a period of approximately 8 min during the shock compression. This suggested that a downward field-aligned current during the preliminary stage of the SI was the main driver of the first plasma flow reversal, and that the subsequent new discrete auroral arc might be associated with field-aligned acceleration in the region of the main impulse related to upward field-aligned currents. Ground magnetometer data suggested that the oscillation of the ionospheric convection on the duskside was associated with field line resonance activity.

The performance of the ZHS HF radar operation was checked using data from 2010 to 2012. The diurnal and seasonal variations of ionospheric echoes and their dependences on geomagnetic activity were analyzed by Hu et al.[42] Statistical studies showed that the occurrence of echoes in different beams varied at different frequencies. It depended on the direction of the beam and on the area over which the beam could achieve the condition of orthogonality between the wave vector and Earth's magnetic field. Diurnal variation was obvious with double-peaked structures both in the occurrence rate and in the average power at 04:00–08:00 and 16:00–17:00 UTC. The spectral widths on the dayside were often higher than on the nightside because of the high-energy particle precipitation in the cusp region. Seasonal variations were more obvious for beams with larger numbers. The occurrence, average power, line-of-sight velocity, and spectral widths were generally larger in winter months than summer months.

Polar mesosphere summer echoes (PMSEs) are strong radar returns from Bragg-scale structures in the polar summer mesosphere (80–90 km altitude) under very low temperatures. Liu et al.[43] reported the first observations of PMSEs by the ZHS SuperDARN radar and presented a statistical analysis of PMSEs from 2010 to 2012. The special features of diurnal variations were observed, of which the maximum was near local midnight and the secondary maximum appeared 1–2 h after local noon. The results showed that auroral particle precipitation plays a non-negligible role in PMSE occurrence.

3.4 Geomagnetic pulsation and space plasma wave

It is generally accepted that electromagnetic ion cyclotron (EMIC) waves are generated around the equatorial regions and that they propagate toward the high-latitude ionosphere in both hemispheres. Liu at al.[44-45] described a prolonged EMIC wave event in the Pc2 (the Type 2 continuous pulsation of geomagnetic pulsations) (0.1–0.2 Hz) frequency band above the He^+ cyclotron frequency detected by the four-satellite Cluster constellation as it traversed sunward from L~13 in the outer magnetosphere to the magnetopause, over 13°–20° magnetic latitude north of the equator and across the high-latitude cusp region near local magnetic noon. The H^+ ion data provided evidence that the waves were generated locally via ion cyclotron instability. It was suggested the off-equatorial minimum magnetic field regions might be important source regions for these waves in the outer magnetosphere.

Liu et al.[46] subsequently analyzed a long-duration EMIC wave event seen in the inner magnetosphere to investigate the propagation characteristics of these waves in the vicinity of the plasmapause. This study took advantage of the south to north orbit of the four-satellite Cluster constellation as it passed through perigee at L~4.2 at approximately 08:00 MLT on 2 November 2001. The observation results of the distribution and of the occurrence of group ray angles are shown in Figures 4(a) and 4(b), respectively. Wave polarization appeared associated with plasma density, with left hand in the equatorial region, right hand at higher latitudes nearer the plasmapause, and a mixture in between. Poynting flux measurements showed that wave energy was directed predominantly along the geomagnetic field lines toward high latitudes in both hemispheres. These results suggest plasma density and its gradient play significant roles in confining the wave source region and in affecting the wave properties, which would help in furthering the understanding of wave generation and propagation mechanisms in the magnetosphere plasma environment.

Using induction magnetometer data from ZHS and the Davis Station in Antarctica obtained in March, June, September, and December 2004, Qiu et al.[47] performed cross-spectrum analysis to undertake a statistical study on Pc1 and Pc2 wave occurrence, center frequency, and amplitude variations with respect to season and magnetic local time. In 2932 valid wave events, Pc1 and Pc2 waves had occurrence of 51.4% in March, 26.1% in September, 18.6% in December, and 3.8% in June. They occurred frequently (59.8%) near magnetic noon, which suggests that Pc1 and Pc2 waves near cusp latitudes are influenced significantly by ionospheric conductivity.

3.5 Space weather in polar regions

Liu et al.[48] used the KRM magnetogram-inversion algorithm, combined with the magnetic record of the Northern Hemisphere to deduce the distribution of the current vector and the electric potential in the polar ionosphere during a substorm event on 13 December 2004. The results showed sudden enhancement of the westward electrojet at the midnight sector after the onset of expansion. The equivalent current system was characterized as a two-vortex structure at the nightside, in association with a southward electric field. All these results indicated the dominant role of the unloading process at the expansion phase. The enhancement of the conductivity was responsible for the increase of the westward electrojet. Liu et al.[49] also reported on four successive substorm events, which followed a nine-hour growth phase on

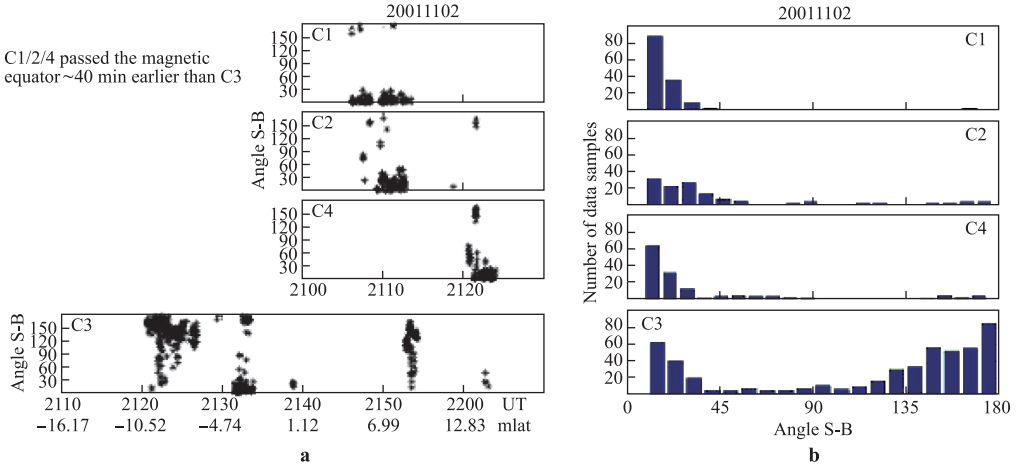

Figure 4 Distribution of group ray angles between the Poynting flux vector of the Pc1 (the Type 1 continuous pulsation of geomagnetic pulsations) waves and the magnetic field direction during 21:00–22:10 UTC on 2 November 2001 (**a**). Occurrence of group ray angles between the Poynting flux vector of the Pc1 waves and the geomagnetic field direction during 21:00–22:10 UTC on 2 November 2002[46] (**b**).

5 December 2008, which were observed by the Time History of Events and Macroscale Interaction during Substorms (THEMIS) and the GOES 11 satellites with simultaneous coverage by the Alaska and THEMIS ground magnetometers. Several interesting and unique features were found for these cases. At least four substorm expansion onsets occurred, including a double-onset event. The latter appears to challenge the reconnection hypothesis for double-onset substorms and instead, it favors an instability mechanism for the onsets that could not be explained by the two neutral line models.

Using observations from multiple instruments, Wu et al.[50] investigated the Arctic ionospheric variations during the main phase of a magnetic storm on 14–15 December 2006 to characterize the effects caused by high-energy particle precipitation. Significant increases in electron density for these different observations were found in the Arctic ionosphere during the main phase of the magnetic storms, as shown in Figure 5. The observations provided direct evidence that storm-time *E*-layer electron density enhancements (e.g., the sporadic *E*) could form nearly dominant proportions of the observed TEC increases. These increases were accompanied by ionospheric absorption enhancement at altitudes of about 90 km. The *Y*-component of the magnetic field to the south of Scandinavian, northwest part of Russia and Svalbard (SNRS) decreased, indicating the presence of a strong upward field-aligned electric current in the Arctic ionosphere. These features were interpreted as effects of high-energy electron precipitation during the magnetic storm, attributable to the substorm reflected on the AL index and the measurements of the IMAGE magnetometer chain.

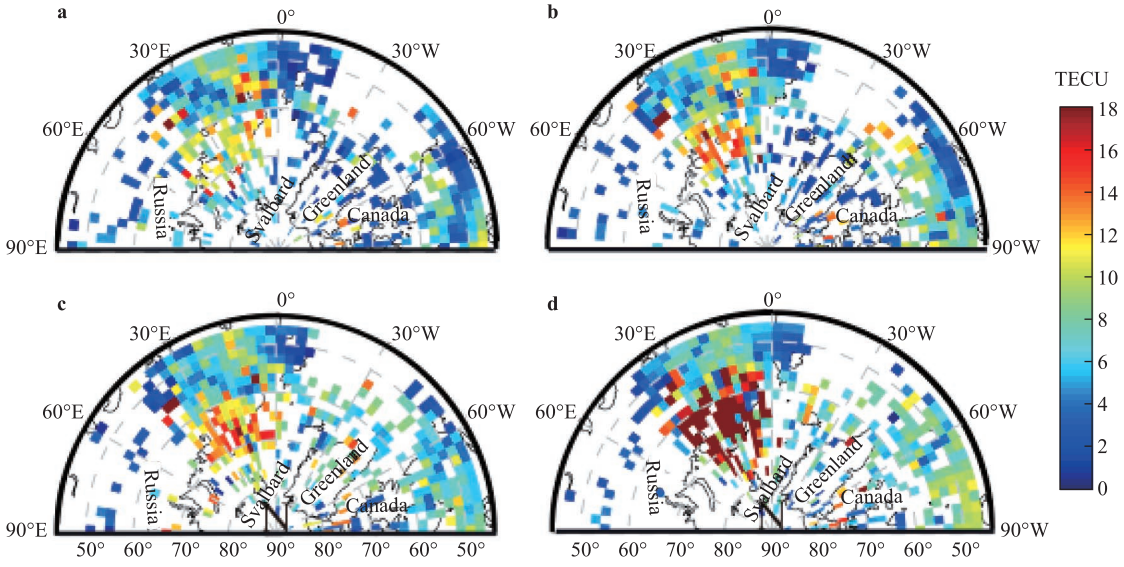

Figure 5 TEC maps of four time frames in the Northern Hemisphere on a geographic grid: **a**, 23:00–23:05 UTC on 14 December; **b**, 23:20–23:25 UTC on 14 December; **c**, 23:40–23:45 UTC on 14 December; **d**, 00:00–00:05 UTC on 15 December, 2006[50].

3.6 Simulations on polar ionosphere-magnetosphere

Yang et al.[51] simulated *F*-region plasma density evolution under the combined effects of soft precipitation and the electric field based on a self-consistent model of the polar ionosphere. The results showed that when the local electric field was >80 mV, effective "breaking off" occurred.

It is also important to evaluate the roles of convection and particle precipitation in the polar *F* region, because it contains plasma structures on the scale of thousands to just several kilometers. Using data recorded by the ESR and at ZHS, the features of the climatological diurnal variation in winter of the solar minimum at cusp latitudes were investigated[52]. Simulations of both hemispheric polar ionospheres for winter were undertaken to try to understand the general statistical features. The simulated results of diurnal variation of NmF2 under different geomagnetic conditions are shown in Figure 6. It was found that the major difference in NmF2 variation between both stations could be explained by the unique location of each station relative to the sunlit demarcation line during the day. For quiet periods, photoionization from lower latitudes contributes to the major peak of NmF2 in the diurnal variation at ZHS, while interaction between horizontal convection and auroral precipitation is the main cause of NmF2 variation observed by the ESR. For active periods, both stations showed an increase of NmF2 attributable to the transportation of higher density plasma from lower latitudes on the dayside with the expansion of the polar cap and additional ionization from soft precipitation of electrons.

4 Summary and prospects

The advantages offered by the unique geographical locations of the Chinese Antarctic GWS, ZHS, and Arctic YRS, CIAO, and KHO stations make them ideally suited for undertaking polar UAP observations and research. With the development of the Chinese Antarctic and Arctic expeditions, new fields

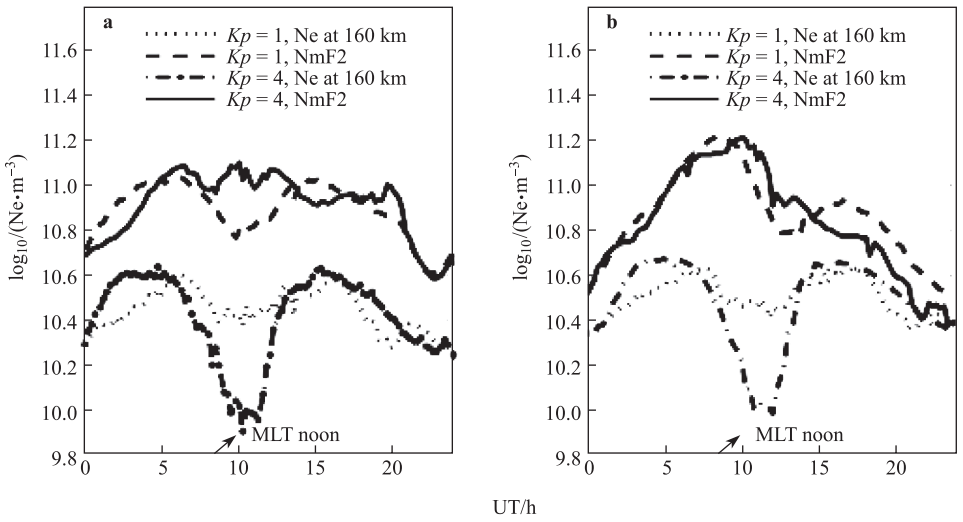

Figure 6 Simulated diurnal variation of NmF2 under quiet (*Kp*=1) and active (*Kp*=4) conditions at (**a**) Svalbard and (**b**) ZHS, respectively[52], where *Kp* is the global geomagnetic storm index.

of research in polar UAP are being exploited. This review focused on the rapid progress made in the last 5 years, the most important highlights of which are summarized in the following.

(1) Two new observatory sites were commissioned: KHO located in the cusp region and CIAO located in the aurora oval region. Several UAP observation instruments have been installed and they have commenced operations.

(2) Direct observations of the full evolution of patches during a geomagnetic storm have been reported. These observations showed the modulation of nightside reconnection helped form the gaps between patches.

(3) Long-term data of diffuse auroras have been surveyed and two categories of DDAs have been classified. Furthermore, the generation of throat aurora has been confirmed and found to occur along open magnetic field lines.

(4) Comprehensive analyses of auroral observations made in the Arctic and Antarctica have been performed, and the characteristics of post-noon auroral bright spots/auroral spirals and the orientations of dayside aurora arc alignments have been reported.

(5) Based on the SuperDARN radar data at ZHS, installed in 2010, the radar's performance was confirmed and it was found that auroral particle precipitation plays an important role in PMSE occurrence.

(6) The temporal characteristics of *F*-lacunae at ZHS were studied and their correlations with associated TEC variations were established.

In 2014, the Scientific Committee on Antarctic Research agreed on the priorities for Antarctic research for the next two decades. The areas of interest were categorized broadly into six scientific themes, one of which is to observe space and the Universe[53]. The focus is on furthering the understanding of high-energy particles from solar flares that are funneled to the poles along Earth's magnetic field lines, and assessing the risk of solar events disrupting global communications and power systems. Moreover, China's 13th Five-Year Plan has clarified that changes in the polar regions and their influences on the climate and the environment will be at the forefront of research in the near future. This means that solar activity, space weather, and climate change will become an inseparable complex subject in polar science. Public awareness of the importance of the solar-terrestrial environment is increasing. Changes in space weather caused by solar storms can have serious effects on human activities, which might provide new challenges and opportunities both in space physics studies and in monitoring and forecasting space weather.

The areas encompassed by polar UAP research in China are being expanded from the ionosphere-magnetosphere to all solar-terrestrial space. Mutual and synchronous development of polar UAP and polar atmospheric sciences will continue, and associated research on the stratosphere, mesosphere, and thermosphere will be undertaken.

Considering the prospects for polar upper-atmospheric research, the following observations are offered.

(1) Geospatial physics considers the behavior of the entire solar-terrestrial system. It is necessary to study solar wind–magnetosphere–ionosphere coupling and auroral dynamics, including the magnetosphere–ionosphere dynamic processes dealing with particle precipitation, field currents, convection fields, plasma waves, auroral characteristics, and their relations to solar wind–magnetosphere interaction. It is essential to examine polar ionosphere coupling to the neutral atmosphere. This includes the polar ionosphere and its relations with solar activities, polar plasma convection and precipitation, its coupling with the middle and lower atmosphere, sudden stratospheric warming events and their relation to the lower ionosphere, and the impact of energetic particle precipitation on Earth's climate system.

(2) Taking advantage of the geographic locations of the Chinese polar stations, it is imperative to investigate inter-hemispheric comparisons of the polar regions, which could

be performed using multi-instrument observations at the geomagnetically conjugate stations.

(3) It is important to strengthen the basic applied research on space weather. Studies are needed on severe space weather events and their relations to solar conditions. The polar ionospheric response to magnetic storms and substorms is also an important research topic. It is critical to learn how solar energy enters the polar upper atmosphere and how polar ionospheric disturbances propagate toward middle and lower latitudes. It is necessary to explore models and methods for space weather prediction and to develop ionospheric models of the polar regions, which will require the construction of global models by synthesizing multi-instrument data using assimilation techniques. It is important to establish the parameters and index systems capable of describing space weather in polar regions.

(4) With the deployment of the Taishan Station (73°51'S, 76°58'E) in Antarctica and CIAO, the Chinese ground-based observational platform has been improved. Future cooperation between China and other Arctic countries in UAP observations will develop our ground-based observational range in the polar regions. This will offer advantageous conditions for an observational network that will expand the monitoring area from the cusp region and auroral zone to the polar cap and subauroral zone. The program for polar-orbiting satellites makes it possible for the development of satellite-based space environment monitoring technology, e.g., the UVI. In addition, it is also very important to plan the monitoring of solar activity and the observation of the middle and upper atmosphere in the polar regions.

Acknowledgments This work was supported by the Chinese Polar Environment Comprehensive Investigation and Assessment Programs (Grant nos. CHINARE 2017-04-01, and 2017-02-04), National Natural Science Foundation of China (Grant nos. 41274164, 41374159, 41431072, and 41274148), Pudong Development of Science and Technology Program (Grant no. Pkj2013-z01), and Top-Notch Young Talents Program of China. The authors acknowledge the use of data from the Chinese Meridian Project and they are grateful to the Chinese National Antarctic and Arctic expeditions for their dedicated efforts in collecting the observational data. The onsite data were issued by the Data-sharing Platform of Polar Science (www.chinare.org.cn) maintained by the Polar Research Institute of China and the Chinese National Arctic and Antarctic Data Center.

References

1 Liu R Y, Yang H G. Progress in polar upper atmospheric physics research in China. Adv Polar Sci, 2012, 23(2): 55–71, doi: 10.3724/SP.J.1085.2012.00055
2 Xu S, Zhang B C, Liu R Y, et al. Comparative studies on ionospheric climatological features of NmF2 among the Arctic and Antarctic stations. J Atmos Solar Terrestr Phys, 2014, 119: 63–70
3 He F, Zhang B C, Moen J, et al. A conjugate study of the polar ionospheric F2-layer and IRI-2007 at 75° magnetic latitude for solar minimum. Adv Polar Sci, 2011, 22(3): 175–183, doi: 10.3724/SP.J.1085.2011.00175
4 He F, Zhang B C, Huang D H. Averaged NmF2 of cusp-latitude ionosphere in northern hemisphere for solar minimum–Comparison between modeling and ESR during IPY. Sci China Tech Sci, 2012, 55(5): 1281–1286, doi: 10.1007/s11431-012-4782-0
5 Xu S, Zhang B C, Liu R Y, et al. The effect of solar activity on the NmF2 at Zhongshan Station. Chin J Polar Res, 2013, 25(2): 142–149 (in Chinese)
6 Yang S G, Zhang B C, Fang H X, et al. F-lacuna at cusp latitude and its associated TEC variation. J Geophys Res, 2014, 119(12): 10384–10396
7 Yang S G, Zhang B C, Fang H X, et al. Study on F-lacuna characteristics at Zhongshan station, Antarctic. Chinese J Geophys, 2016, 59(1): 8–16 (in Chinese)
8 Wu Y W, Liu R Y, Zhang B C, et al. Characteristics of the E-layer dominated ionosphere in the polar regions during polar nights. Chin J Polar Res, 2013, 25(2): 132–141 (in Chinese)
9 Cai H T, Li F, Shen G, et al. E layer dominated ionosphere observed by EISCAT/ESR radars during solar minimum. Ann Geophys, 2014, 32(10): 1223–1231
10 He F, Hu H Q, Hu Z J, et al. A new technique for deriving the quiet day curve from imaging riometer data at Zhongshan Station, Antarctic. Sci China Tech Sci, 2014, 57(10): 1967–1976
11 Tanaka Y, Makita K, Nishino M, et al. Development of data analysis program for imaging riometer by using MATLAB. Bull Sci Eng, Tankushoku Univ, 2007, 10(1): 61–66 (in Japanese)
12 He F, Hu H Q, Yang H G, et al. A comparative study of the cosmic noise absorption Keograms generated by two different quiet day curve techniques. Chinese J Geophys, 2015, 58(1): 1–11 (in Chinese)
13 Liu Q Q, Hu H Q, Lv J Y, et al. Case study on nightside polar ionospheric convection response to interplanetary shock. Chin J Space Sci, 2017, 37(2): 140–150 (in Chinese)
14 Li P H, Hu H Q, Fang H X, et al. Statistical properties of polar ionospheric scintillations at the South Pole and Mcmurdo stations, Antarctica. Chin J Polar Res, 2016, 28(1): 19–24 (in Chinese)
15 An J C. Ionospheric tomography algorithms and their applications in polar area. Wuhan: Wuhan University, 2011
16 An J C, Wang Z M, Li F, et al. Behavior of Weddell Sea Anomaly observed by ground-based GPS. Progress in Geophys, 2014, 29(3): 993–998 (in Chinese)
17 Meng Y, An J C, Wang Z M, et al. Spatial distribution of Antarctic ionosphere TEC based on GPS. Acta Geodaet Cartogr Sinica, 2011, 40(1): 37–40 (in Chinese)
18 Liu J B, Chen R Z, An J C, et al. Spherical cap harmonic analysis of the Arctic ionospheric TEC for one solar cycle. J Geophys Res, 2014, 119(1): 601–619
19 Deng Z X, Feng J, Zhen W M, et al. Variations of ionospheric TEC surrounding great wall station, Antarctica. Chin J Radio Sci, 2015, 30(5): 951–958 (in Chinese)
20 Xing Z Y, Yang H G, Han D S, et al. Poleward moving auroral forms (PMAFs) observed at the Yellow River Station: a statistical study of its dependence on the solar wind conditions. J Atmos Solar, 2012, 86: 25–33
21 Xing Z Y, Yang H G, Wu Z S, et al. A parameter model of auroral emissions and particle precipitation near magnetic noon. Chinese J Geophys, 2013, 56(7): 2163–2170 (in Chinese)
22 Xing Z Y, Yang H G, Han D S, et al. Dayside poleward moving auroral forms and ionospheric convection under stable interplanetary magnetic field (IMF) conditions. Sci China Technol Sci, 2013, 56(4): 910–916
23 Hu Z J, Yang H G, Hu H Q, et al. The hemispheric conjugate observation of postnoon "bright spots"/auroral spirals. J Geophys Res, 2013, 118(4): 1428–1434
24 Hu Z J, Ebihara Y, Yang H G, et al. Hemispheric asymmetry of the structure of dayside auroral oval. Geophys Res Lett, 2014, 41(24):

8696–8703
25 Shi R, Hu Z J, Ni B B, et al. Modulation of the dayside diffuse auroral intensity by the solar wind dynamic pressure. J Geophys Res, 2014, 119(12): 10092–10099
26 Han D S, Chen X C, Liu J J, et al. An extensive survey of dayside diffuse aurora based on optical observations at Yellow River Station. J Geophys Res, 2015, 120(9): 7447–7465
27 Han D S, Nishimura Y, Lyons L R, et al. Throat aurora: the ionospheric signature of magnetosheath particles penetrating into the magnetosphere. Geophys Res Lett, 2016, 43(5): 1819–1827
28 Han D S, Hietala H, Chen X C, et al. Observational properties of dayside throat aurora and implications on the possible generation mechanisms. J Geophys Res, 2017, 122(2): 1853–1870
29 Qiu Q, Yang H G, Lu Q M, et al. Orientation variation of dayside auroral arc alignments obtained from all-sky observation at yellow river station, Svalbard. J Atmos Solar, 2016, 142: 20–24
30 Qiu Q, Yang H G, Lu Q M, et al. Motion of dayside auroral arc observed at Yellow River Station affected by the earth's rotation. Chin J Space Sci, 2016, 36(6): 909–915 (in Chinese)
31 Ni B B, Thorne R M, Zhang X J, et al. Origins of the Earth's diffuse auroral precipitation. Space Sci Rev, 2016, 200(1–4): 205–259
32 Liu J J, Hu H Q, Han D S, et al. Response of nightside aurora to interplanetary shock from ground optical observation. Chinese J Geophys, 2013, 56(5): 1785–1796 (in Chinese)
33 Liu J J, Hu H Q, Han D S, et al. Simultaneous ground-based optical and SuperDARN observations of the shock aurora at MLT noon. Earth, Planets Space, 2015, 67: 120
34 Huang D H, Hu H Q, Liu Y, et al., Cosmic ray observation at Antarctic Zhongshan Station. Chin J Space Sci, 2016, 36: 897–903 (in Chinese)
35 Zhang Q H, Liu R Y, Yang H G, et al. SuperDARN CUTLASS Finland radar observations of high-latitude magnetic reconnections under northward interplanetary magnetic field (IMF) conditions. Sci China Technol Sci, 2012, 55(5): 1207–1216
36 Zhang Q H, Zhang B C, Lockwood M, et al. Direct observations of the evolution of polar cap ionization patches. Science, 2013, 339(6127): 1597–1600
37 Zhang Q H, Zhang B C, Moen J, et al. Polar cap patch segmentation of the tongue of ionization in the morning convection cell. Geophys Res Lett, 2013, 40(12): 2918–2922
38 Zhang Q H, Dunlop M W, Lockwood M, et al. Inner plasma structure of the low-latitude reconnection layer. J Geophys Res, 2012, 117(A8): A08205
39 Yang S G, Zhang B C, Fang H X, et al. New evidence of dayside plasma transportation over the polar cap to the prevailing dawn sector in the polar upper atmosphere for solar-maximum winter. J Geophys Res, 2016, 121(6): 5626–5638
40 Liu E X, Hu H Q, Liu R Y, et al. Diurnal variation of the HF radar echoes at Zhongshan Station and the influence of geomagnetic activity. Chinese J Geophys, 2012, 55(9): 3066–3076 (in Chinese)
41 Liu J J, Hu H Q, Han D S, et al. Optical and SuperDARN radar observations of duskside shock aurora over Zhongshan Station. Adv Polar Sci, 2013, 24(1): 60–68
42 Hu H Q, Liu E X, Liu R Y, et al. Statistical characteristics of ionospheric backscatter observed by SuperDARN Zhongshan radar in Antarctica. Adv Polar Sci, 2013, 24(1): 19–31
43 Liu E X, Hu H Q, Hosokawa K, et al. First observations of polar mesosphere summer echoes by SuperDARN Zhongshan radar. J Atmos Solar, 2013, 104: 39–44
44 Liu Y H, Fraser B J, Menk F W. Pc2 EMIC waves generated high off the equator in the dayside outer magnetosphere. Geophys Res Lett, 2012, 39(17): L17102
45 Liu Y H, Fraser B J, Menk F W, et al. Correction to "Pc2 EMIC waves generated high off the equator in the dayside outer magnetosphere", Geophys Res Lett, 2013, 40(10): 1950–1951
46 Liu Y H, Fraser B J, Menk F W, EMIC waves observed by Cluster near the Plasmapause. J Geophys Res, 2013, 118(9): 5603–5615
47 Qiu Y T, Liu Y H, Zhao H F. Statistical characteristics of Pc1–2 waves near the cusp latitudes. Chin J Polar Res, 2014, 26(3): 324–330 (in Chinese)
48 Liu J M, Zhang B C, Kamide Y, et al. Electrodynamics in the polar ionosphere during the IMF-north substorm on 13 December 2004. Chin J Space Sci, 2012, 32(1): 20–24 (in Chinese)
49 Liu J M, Kamide Y, Zhang B C, et al. THEMIS and ground-based observations of successive substorm onsets following a super-long growth phase. Ann Geophys, 2013, 31(5): 835–843
50 Wu Y W, Liu R Y, Zhang B C, et al. Multi-instrument observations of plasma features in the Arctic ionosphere during the main phase of a geomagnetic storm in December 2006. J Atmos Solar, 2013, 105–106: 358–366
51 Yang S G, Zhang B C, Zhang Q H, et al. Numerical simulation of the role of dayside magnetic reconnection in polar cap patch formation. Chinese J Geophys, 2014, 57(6): 771–777
52 Zhang B C, Yang S G, Xu S, et al. Diurnal variation of winter F region ionosphere for solar minimum at both Zhongshan Station, Antarctica, and Svalbard Station, Arctic. J Geophys Res, 2015, 120(11): 9929–9942
53 Kennicutt II M C, Chown S L, Cassano J J, et al. Polar research: six priorities for Antarctic science. Nature, 2014, 512(7512): 23–25